Meccanica (2022) 57:2473–2491
https://doi.org/10.1007/s11012-022-01586-6

An investigation of fluid-structure interaction in pipe conveying flow using reduced-order models

João D. B. dos Santos · Gustavo R. Anjos · Marcelo A. Savi

Received: 31 January 2022 / Accepted: 1 September 2022 / Published online: 14 September 2022

Abstract Fluid-structure interactions are essential to be evaluated in pipelines where the fluid dynamics induces structural vibrations that need to be properly investigated for engineering design. The flow of internal fluids can be laminar or turbulent, which makes such analysis a complex task. This paper investigates the analysis of Fluid-structure interaction from reduced-order models where a Bernoulli–Euler beam is employed to represent the pipe while fluid dynamics is represented by nonlinear oscillators. Structural analysis employs the Galerkin method for spatial discretization. Fluid dynamics is described by considering van der Pol oscillator together with the Langevin equation. In this regard, laminar and turbulent responses are described. Results show that the reduced-order model allows one to replicate the frequency spectrum of the pipeline response considering the parametric variation of the flow velocity and stochastic fluctuations. Nonlinear dynamics perspective shows to be interesting representing instabilities and some complex responses as limit cycle behavior.

J. D. B. dos Santos · G. R. Anjos · M. A. Savi (✉)
COPPE - Department of Mechanical Engineering, Center for Nonlinear Mechanics, Universidade Federal Do Rio de Janeiro, P.O. Box – 68.503, Rio de Janeiro, RJ 21941-972, Brazil
e-mail: savi@mecanica.coppe.ufrj.br

J. D. B. dos Santos
e-mail: joao.deodato@coppe.ufrj.br

G. R. Anjos
e-mail: gustavo.rabello@coppe.ufrj.br

Keywords Fluid-structure interaction · Flow-induced vibration · Pipe conveying fluid · Stochastic fluctuation · Langevin's model · Nonlinear dynamics

1 Introduction

Fluid transport pipelines are used in various branches of engineering such as water, steam, oil and gas. Fluid dynamics induce vibrations that need to be properly analyzed on the pipeline design. In this regard, the description of the Fluid-structure interactions is essential for the analysis of pipelines. Païdoussis et al. [17] presented a discussion about this subject by describing the mechanisms of Fluid-structure interaction, the reasonable assumptions chosen to simplify the analysis and several results for structure vibrations due to internal and external flows, showing that displacement amplitude can reach significant values due to flow conditions as those induced by turbulent effects. External flows are characterized by fluid motion that is not confined by any surface, and therefore, the influence of pressure and velocity fields into immersed bodies and their vibration are investigated through lift and drag forces acting on their surfaces. On the other hand, internal flows are those confined by any surface, such as found in pipelines and cooling systems.

Fluid flow is described by the Navier–Stokes equations and, in general, the flow can be either laminar or turbulent, which makes its description a complex

task. The difficulties to treat Navier–Stokes equations motivate the use of reduced-order models that are useful for different goals. Aranha [1] presented analytical argues showing that a fluid-elastic oscillator can be used to model asymptotic solutions of the Navier–Stokes equations in slender bodies, allowing the description of different flow regimes beyond the critical Reynolds number. Orsino et al. [16] investigated the use of the modular modeling methodology for a class of Fluid-structure interaction by proposing a planar nonlinear reduced-order model for a submerged cantilevered pipe ejecting fluid under vortex induced vibration (VIV) and numerical simulations to provide the response of the model.

Postnikov et al. [21] presented a new two degrees-of freedom wake oscillator model based on the van der Pol equation, successfully employed to describe VIV in cylinders subjected to cross-flow and in-line flow conditions. Experimental and numerical data were used to calibrate the model and to verify the predictions of Fluid-structure interactions. Kurushina et al. [9] and Pavlovskaia et al. [19] presented the modeling of VIV using reduced-order models through a set of wake oscillator with different types of nonlinear dissipation. The slender body is modeled as Euler–Bernoulli beam, while the main flow is modeled as van der Pol oscillators. Two configurations of flow were studied relative to their positions and conclusions point that the vibration level at low frequencies were reasonably well predicted by the simulations. Franzini and Bunzel [5] investigated the dynamics of a rigid cylinder mounted on elastic supports connected to piezoelectric harvesters and subjected to the VIV phenomenon. The main objective was to highlight the influence of an additional structural degree of freedom on the dynamics of the Fluid-structure-electric system, discussing a sensitivity analysis.

Ueno [25] analyzed VIV phenomenon establishing the effectiveness of a particular class of nonlinear vibration absorbers (NVA) as a passive suppressor of rigid cylinders mounted on elastic supports. A parametric study showed the influence of the suppressor mass on the VIV suppression. Gonçalves et al [6] developed spectral analysis methods to numerically investigate VIV mechanisms, improving the statistics analysis available in the literature. The authors concluded that the Hilbert–Huang transform method is more reliable than the traditional methods available due to the larger number of points to calculate the statistics characteristics. Experimental investigation was conducted by Korkischko and Meneghini [8] analyzing the effect of the geometric parameters of helical strakes on VIV in isolated circular cylinders. The authors concluded that the strakes do not increase the magnitude of the out-of-plane velocity compared to the isolated plain cylinder. A study of wake oscillator with frequency dependent coupling is presented by Ogink and Metrikine [15] to improve the modeling of VIV of an elastically mounted cylinder in fluid flow. Several attempts to model VIV using oscillators is presented showing the difficulties to find one set of frequency dependent coefficients that conforms the forced vibration experiments at all amplitudes of cylinder motion using van der Pol equation. Additionally, nonlinear effects of the wake oscillator do not model VIV measurements with accuracy.

A model using a linear equation to describe pipe transverse vibrations induced by internal flow and vortexes caused by external cross flow is presented by Meng et al. [12]. Sazesh and Shams [23] applied the stochastic approach to a cantilever pipe with fluid flow induced vibration. Dynamical analysis and stability of a multi-span pipe conveying fluid is treated by El-Sayed and El-Mongy [4] using a variational based method. Free vibration of viscoelastic pipes using the multi-scale method is investigated by Tang et al. [24].

Loiseau et al. [10] presented an alternative reduce-order modeling framework based on experimental data. In this regard, complex fluid dynamics are modeled by a grey-box modeling procedure that is able to captures the main features of nonlinear fluid flow.

Moreover, several phenomena are important for a proper description of the Fluid-structure interaction, including interesting analyses as for instance: the influence of variable density fluid transport on the vibration of rocker pipes [2],the nonlinear dynamics of a pipe interacting with two support walls for different flow speed, considering different kinds of response [13],the experimental and numerical investigations of the vibration of bi-embedded pipes statically deformed subjected to internal flow [3],and the synchronization of two equivalent fluid transport pipes coupled by non-linear springs [11].

The Galerkin method is usually employed to perform the spatial discretization of the partial differential equations that governs Fluid-structure interaction

[3, 11, 13, 14, 23]. Nevertheless, other numerical approaches are employed in different situations as the generalized integral transformation technique to investigate the effect of the proportion between length and diameter on the dynamics of a fluid transport pipe [7]. A probabilistic model for Fluid-structure interaction considering modeling errors is employed to analyze the stability and reliability of the stochastic system [22].

Based on the literature review, it is noticeable that there is a broad literature related to Fluid-structure interactions due to external flows. The use of reducer-order models is of special interest due to its good cost-benefit relation for several applications. Nevertheless, the use of the reduced models is restricted to some specific conditions and the description of internal flow is investigated in few references. This paper deals with the analysis of Fluid-structure interaction considering reduced-order models for internal flows. Pipeline is treated by considering a Euler–Bernoulli beam based on the Païdoussis model. The Galerkin method is employed for spatial discretization. Fluid flow dynamics is described by considering nonlinear oscillators, employing van der Pol oscillators together with Langevin equation. This novel reduced-order model allows the description of different flow regimes with velocity fluctuations, including the turbulent flow description. Numerical simulations are carried out showing the influence of system parameters on the Fluid-structure interaction, evaluating the system stability.

This article is organized as follows. Section 2 presents the governing equations of the Fluid-structure interaction to describe the tube vibration induced by the internal flow. The Galerkin method is used for spatial discretization, assuming the selection of base functions based on vibration modes. Reduced-order models to describe the effect of the fluid flow are presented incorporating the Langevin model to represent the turbulent flow velocity. Afterward, Sect. 3 presents numerical simulations evaluating different fluid flow conditions. Section 4 presents the conclusions.

2 Fluid-structure interaction

Consider a pipe structure represented by a clamped–clamped beam with inner flow-induced vibration, as can be seen schematically in Fig. 1. The structure has a length L and inner diameter D; a transversal displacement is represented by U while the fluid flow is characterized by an arbitrary fluid velocity V and acceleration $\dot{V}$. By considering that $m_t$andρA_f are the mass per unit length respectively of the tube and the fluid, A_f is the tube cross sectional area where ρ is the fluid with density, $\overline{T}$ is the axial tension applied to tube by supports and $\overline{p}$ is the fluid pressure, the governing equations for the structure system that interacts with the fluid are written as follow [18],

$$\begin{aligned} &EI\frac{\partial^4 U}{\partial x^4} + \left(m_t + \rho A_f\right)\frac{\partial^2 U}{\partial t^2} + 2\rho A_f V\frac{\partial^2 U}{\partial x \partial t} \\ &+\left\{\rho A_f V^2 - \overline{T} + A_f\overline{p}\left(1-2\mu_p\right) - \left[\left(m_t+\rho A_f\right)g - \rho A_f\dot{V} - \frac{1}{2}\rho D V^2 C_T\right](L-x)\right\}\frac{\partial^2 U}{\partial x^2} \\ &+\left[\frac{1}{2}\rho D V^2 C_N + \left(m_t+\rho A_f\right)g\right] \\ &\frac{\partial U}{\partial x} + \left[\frac{1}{2}\rho D\left(C_N V + C_d\right)\right]\frac{\partial U}{\partial t} = 0 \end{aligned} \tag{1}$$

where t is time, x is the axial coordinate; E is the elastic modulus, I is the moment of inertia, μ_p is Poisson's ratio, C_d is a drag coefficient, C_T is the longitudinal viscous coefficient, C_N is the normal viscous coefficient, and g is the gravity acceleration. The

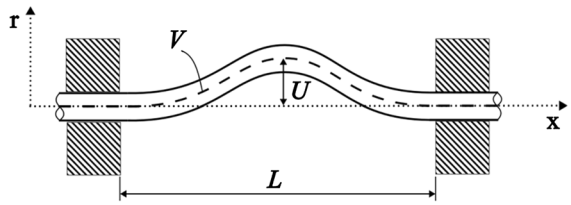

Fig. 1 A fluid conveying pipe with clamped–clamped boundary condition

non-dimensional form of the governing equation can be expressed as follows,

$$\frac{\partial^4\eta}{\partial\xi^4}+\frac{\partial^2\eta}{\partial\tau^2}+2\beta^{1/2}v\frac{\partial^2\eta}{\partial\xi\partial\tau}+\left(\gamma-\frac{1}{2}\varepsilon c_n v^2\right)\frac{\partial\eta}{\partial\xi}+\left\{v^2-\Gamma+\Pi(1-2\mu_p)-\left[\gamma-\beta^{1/2}\dot{v}-\frac{1}{2}\varepsilon c_T v^2\right](1-\xi)\right\}\frac{\partial^2\eta}{\partial\xi^2}+\left[\frac{1}{2}\varepsilon\beta^{1/2}(c_n v+c_d)\right]\frac{\partial\eta}{\partial\tau}=0 \quad (2)$$

with the definitions of following dimensionless parameters,

$$\eta=\frac{U}{L};\ \xi=\frac{x}{L};\ \tau=\left(\frac{EI}{m_t+\rho A_f}\right)^{1/2}\frac{t}{L^2};\ v=\left(\frac{\rho A_f}{EI}\right)^{\frac{1}{2}}LV;\ \varepsilon=\frac{D}{L};$$
$$\beta=\frac{\rho A_f}{m_t+\rho A_f};\ \gamma=\frac{(m_t+\rho A_f)L^3}{EI}g;\ \Gamma=\frac{\overline{T}L^2}{EI};\ \Pi=\frac{A_f\overline{p}L^2}{EI} \quad (3)$$
$$c_N=\frac{4C_N}{\pi};\ c_T=\frac{4C_T}{\pi};\ \kappa=\frac{cL^2}{\left[EI(m_t+\rho A_f)\right]^{1/2}}$$

2.1 Structure spatial discretization

The Galerkin's method is employed to promote a spatial discretization of the governing equations. In essence, it is performed a separation of variables, defining temporal and spatial coordinates [23],

$$\eta(\xi,\tau)=\sum_{j=1}^{j=n}\theta_r(\tau)\phi_r(\xi) \quad (4)$$

where $\theta_r(\tau)$ are the generalized coordinates and $\phi_r(\xi)$ are the eigenfunctions of a beam equation given by

$$\phi_r(\xi)=\cos\lambda_r\xi-\cosh\lambda_r\xi-\frac{\cosh\lambda_r-\cos\lambda_r}{\sinh\lambda_r-\sin\lambda_r}(\sinh\lambda_r\xi-\sin\lambda_r\xi) \quad (5)$$

where λ_r are the dimensionless beam eigenvalues. By assuming clamped–clamped boundary conditions,

$$\eta(0,\tau)=0;\eta(1,\tau)=0$$
$$\frac{\partial\eta}{\partial\xi}(0,\tau)=0;\frac{\partial\eta}{\partial\xi}(1,\tau)=0 \quad (6)$$

On this basis, a set of ordinary differential equations may be arranged in matrix form, resulting in the following discrete system:

$$M\ddot{\theta}+B\dot{\theta}+K\theta=0 \quad (7)$$

where $\theta=\{\theta_1,\theta_2,\ldots,\theta_n\}^T$ and the global matrices of inertia (M), damping (B), and stiffness (K), are built elementwise according to the following local matrix components

$$M_{sr}=\delta_{sr}$$
$$B_{sr}=\left[\frac{1}{2}\varepsilon\beta^{1/2}(c_n v+c_d)+\kappa\right]\delta_{sr}+2\beta^{1/2}vd_{sr}$$
$$K_{sr}=\left[\lambda_r^4\right]\delta_{sr}+\left[v^2-\Gamma+\Pi(1-2\mu_p)\right]e_{sr}+\left[\gamma-\beta^{1/2}\dot{v}-\frac{1}{2}\varepsilon c_T v^2\right](f_{sr}-e_{sr})+\left[\gamma-\frac{1}{2}\varepsilon c_n v^2\right]d_{sr} \quad (8)$$

Here, δ_{sr} represents the Kronecker's delta and the constants d_{sr}, e_{sr} and f_{sr} are given by:

$$d_{sr}=\int_0^1\phi_s\phi_r'd\xi;\ e_{sr}=\int_0^1\phi_s\phi_r''d\xi;\ f_{sr}=\int_0^1\phi_s\xi\phi_r''d\xi \quad (9)$$

2.2 Fluid flow

Fluid-structure interaction is related to the fluid flow characteristics that can be decomposed into random arbitrary pressure and boundary layer pressure fields that appear due pressure–velocity coupling in fluid

flows. The former is related to the velocity fluctuations found in turbulent flows whereas the latter is due to the presence of the fluid boundary layer and the shear stress caused by fluid viscosity. Although the fluid flow is described by the Navier–Stokes equations, the difficulties to treat these equations motivate the use of reduced-order models. Païdoussis [18] classified fluid-induced vibrations based on sources of excitations that include external, movement and instability excitations.

The reduced order model proposed in this work considers the fluid flow velocity to be a combination of a mean flow velocity $\overline{v}$, a time-dependent oscillation function $q(\tau)$, and a stochastic fluctuation v^f. For the sake of simplicity, a homogeneous isotropic turbulence is assumed resulting in a situation where velocity fluctuation v^f is equal in all directions. Therefore, the fluid flow velocity is defined as follows:

$$v = \overline{v}(1 + aq) + v^f \tag{10}$$

where a is an oscillation amplitude. The use of reduced-order models is an interesting approach due to its low computational cost, but of course, should be used with care and observing the validity range for each application. In this regard, Langevin and van der Pol equations are employed to describe fluid flow dynamics.

Langevin equation is widely employed to represent fluctuations on systems described by macroscopic perspective. Random terms are employed to represent the fluctuation sources. On this basis, fluid dynamics is described by stochastic velocity fluctuations, v^f, which allows the representation of either laminar or turbulent flow.

On the other hand, time dependent flow is represented by nonlinear oscillators, specifically, van der Pol oscillator, characterized by a limit cycle behavior. Several natural systems present the limit cycle behavior, a nonlinear phenomenon that represents self-sustained oscillations, represented by an isolated closed orbit on the space state. This behavior has shown to be useful to represent fluid flow [5, 9, 16, 19, 21].

In this regard, the stochastic fluctuation velocity v^{f} is governed by the Langevin equation that considers that fluid particle is subjected to a deterministic drag force and a fluctuation stochastic force, being given by [20]:

$$\dot{v}^f = -\frac{3}{4}C_0\frac{\epsilon_T}{\varphi_k}v^f + \left(C_0\epsilon_T\right)^{1/2}\zeta \tag{11}$$

where the constant $C_0 = 2.1$ is the Kolmogorov constant in such a way that the Langevin's equation is quantitatively consistent with the Kolmogorov hypothesis. In addition, $\zeta \sim \left(\overline{\zeta}, \sigma\right)$ is a standardized random Gaussian variable with a mean value $\overline{\zeta}$ of and a standard deviation σ, φ_k represent the turbulent kinetic energy while ϵ_T represents the turbulent dissipation, both defined as follow.

$$\varphi_k = \frac{3}{2}v^* v^* \epsilon_T = \frac{{\varphi_k}^2}{\nu_k Re_T} \tag{12}$$

Here v^* is an input parameter that represents the flow velocity fluctuation amplitude, ν_k is the kinematic viscosity, usually considered as $\nu_k = 1 \times 10^{-6}\mathrm{m}^2/\mathrm{s}$, Re_T is the turbulence Reynolds number, defined in such a way that the maximum amplitude of the flow velocity fluctuation is limited to 5% or 10% of the mean flow velocity. Note that non-deterministic fluctuation is defined from a Gaussian random number where $\overline{\zeta} = v^*$.

The time-dependent oscillation function q is described by the van der Pol oscillator governed by the following equation, that presents a nonlinear dissipation term, being excited by the structure variable that represents the Fluid-structure coupling,

$$\ddot{q} + \chi\omega\left(q^2 - 1\right)\dot{q} + \omega^2 q = \alpha\ddot{\eta} \tag{13}$$

where ω is dimensionless pulsation frequency employed to characterize fluid flow; χ is a nonlinear dissipation and α is a Fluid-structure coupling coefficient. A simplified version of the fluid flow

Table 1 System parameters

Parameters	Value
ϵ	0.000052
β	0.27
Γ	9800.72
Π	16,651.16
γ	0.5
c_n	1.4
c_T	0.7
c_d	0.1
μ_d	0.3
τ	$0.00036t$

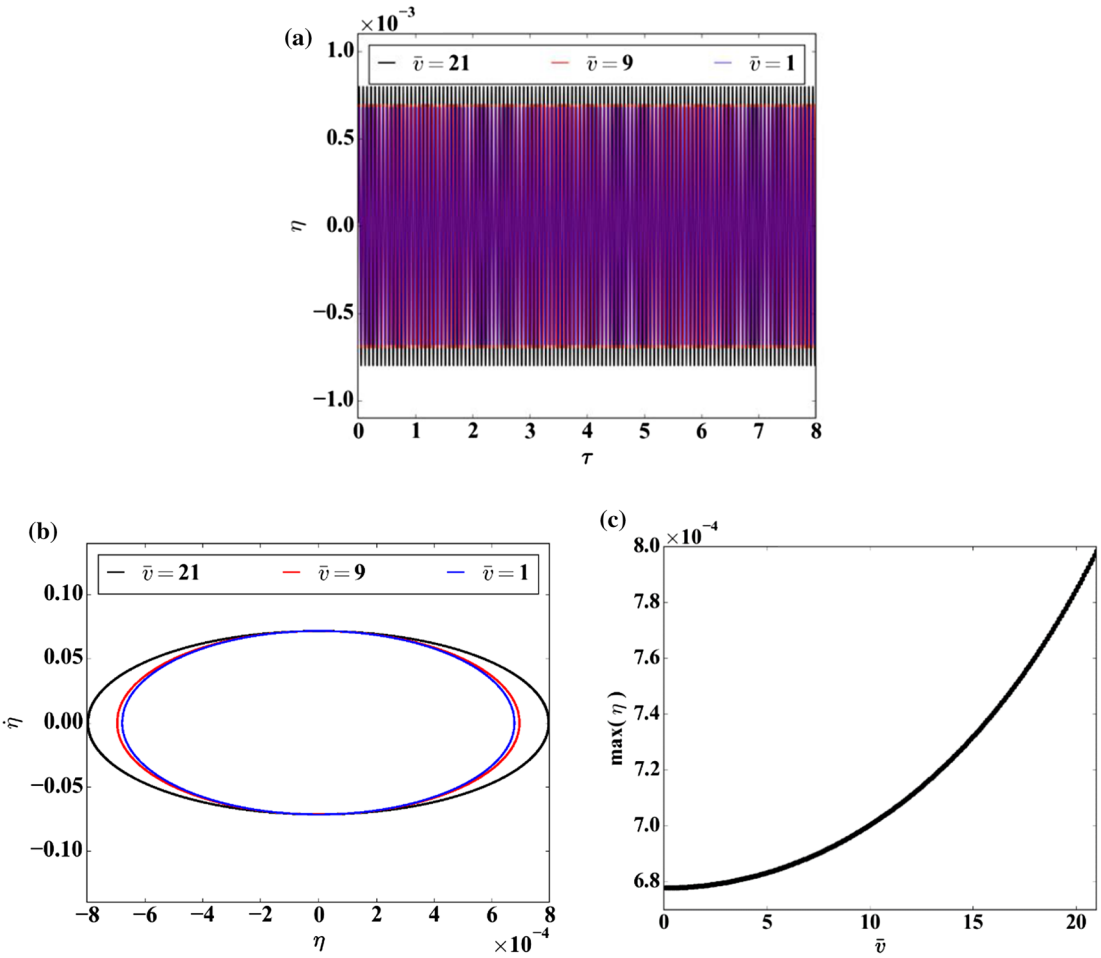

Fig. 2 Fluid-structure dynamical behavior with constant fluid flow velocity. **a** Time history of the structure displacement; **b** structure state space; **c** maximum displacement as a function of the mean flow velocity. The increase of the mean flow velocity causes a reduction of structure frequency oscillation and an increase in the displacement amplitude

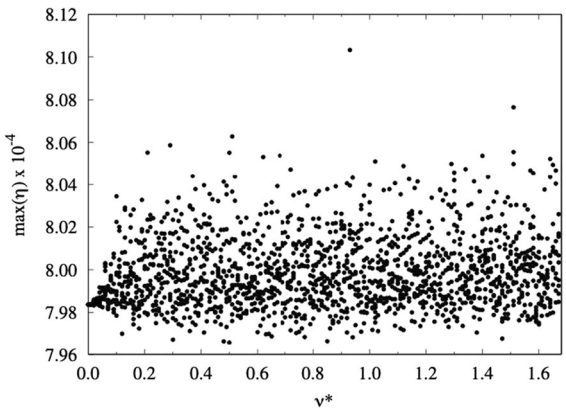

Fig. 3 Influence of the oscillation velocity amplitude considering a fluid with stochastic turbulence in the relative maximum displacement. The amplitude displacement dispersion increases as the turbulence intensity rises

description can be treated by assuming a sinusoidal response where the flow oscillation frequency is independent of the average flow velocity. This means that $\chi = 0$ and $\alpha = 0$, being expressed by

$$q = \sin(\omega\tau) \tag{14}$$

2.3 Governing equations

This section presents a summary of the Fluid-structure interaction governing equations, discussed in the preceding sections. It is assumed a one-degree of freedom oscillator to represent the structure dynamics, which means that a frequency range is being

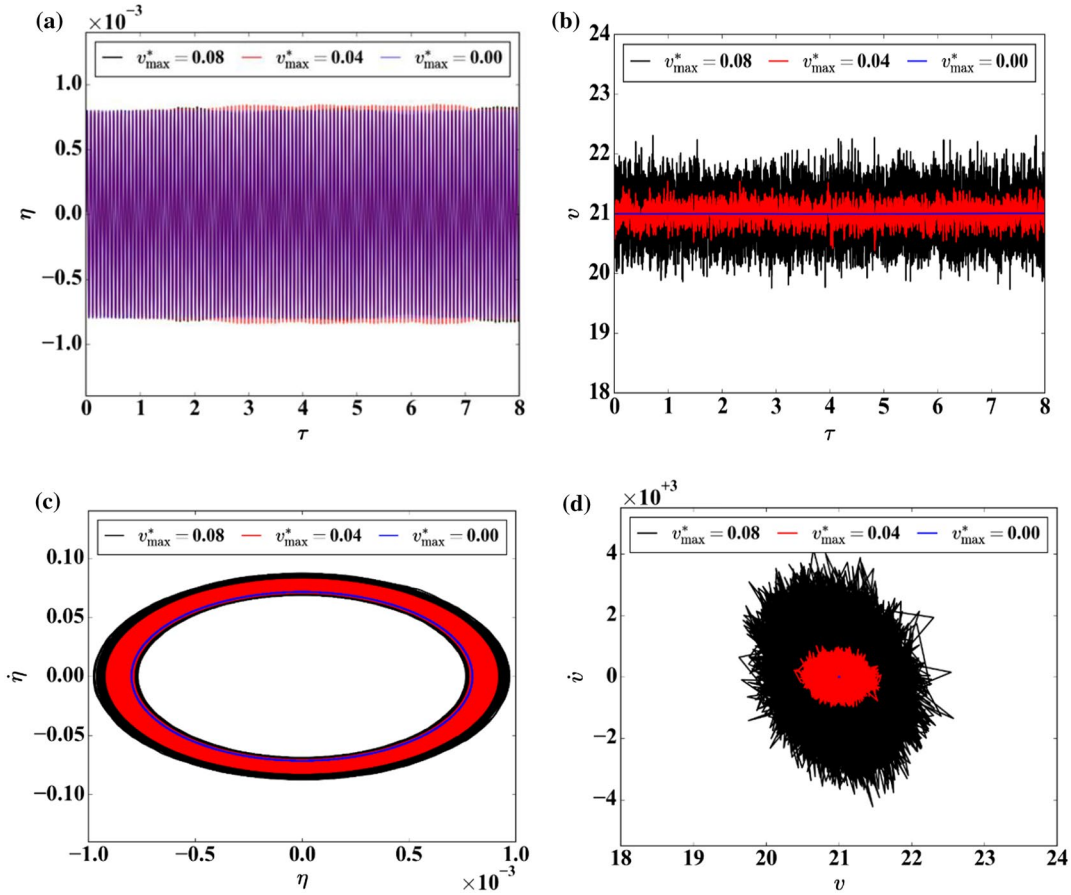

Fig. 4 Fluid-structure dynamical behavior considering a fluid with stochastic fluctuations. **a** Time history of the structure displacement; **b** time history of the flow velocity; **c** structure state space; **d** flow velocity state space

defined for the analysis. Therefore, by considering η as the structure displacement, $\dot{\eta}$and$\ddot{\eta}$ respectively representing velocity and acceleration, the following set of dimensionless equations of motion governs the Fluid-structure interaction:

$$\ddot{\eta} + \left(b_0 + b_1 v\right)\dot{\eta} + \left(k_0 + k_1 v^2 + k_2 \dot{v}\right)\eta = 0 \tag{15}$$

$$v = \overline{v}(1 + aq) + v^f \tag{16}$$

$$\dot{v}^f = -\frac{3}{4} C_0 \frac{\epsilon_T}{\varphi_k} v^f + \left(C_0 \epsilon_T\right)^{1/2} \zeta \tag{17}$$

$$\ddot{q} + \chi\omega\left(q^2 - 1\right)\dot{q} + \omega^2 q = \alpha\ddot{\eta} \tag{18}$$

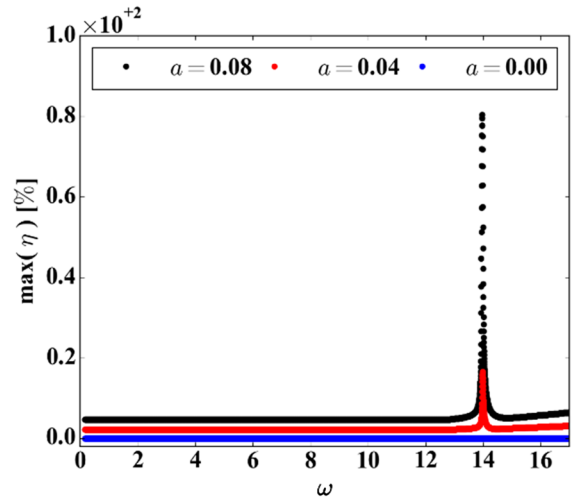

Fig. 5 Frequency response of the Fluid-structure interaction behavior considering a sinusoidal fluid flow, relative maximum displacement

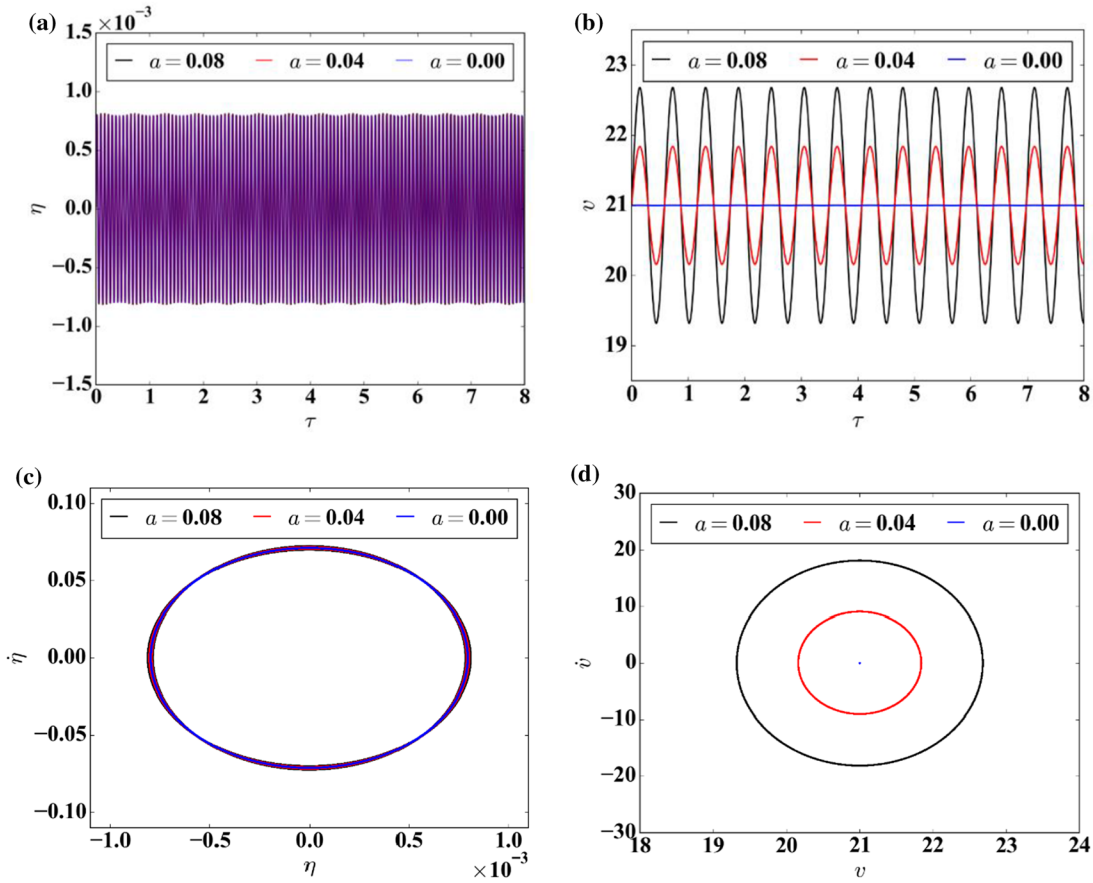

Fig. 6 Fluid-structure dynamical behavior with sinusoidal flow velocity. **a** Time history of the structure displacement; **b** time history of the flow velocity; **c** structure state space; **d** flow velocity state space

where b_0 and b_1 are the dissipation coefficients and k_0, k_1 and k_2 are stiffness coefficients when Eqs. (7, 8) are reduced the first vibration mode, which represents a one-degree of freedom mechanical oscillator associated with the following coefficients,

$$b_0 = \left[\frac{1}{2}\varepsilon\beta^{1/2}c_d + \mu_d\right] \tag{19}$$

$$b_1 = \left[\frac{1}{2}\varepsilon\beta^{1/2}c_n\right] + 2\times 10^{-3}\beta^{1/2} \tag{20}$$

$$k_0 = 500.55 - 13.52\left[-\Gamma + \Pi\left(1-2\mu_p\right)\right] + 6.76\gamma \tag{21}$$

$$k_1 = -13.52 - 6.76\left[\frac{1}{2}\varepsilon c_T\right] - \left[\frac{1}{2}\varepsilon c_n\right]\times 10^{-3} \tag{22}$$

$$k_2 = -6.76\beta^{1/2} \tag{23}$$

3 Numerical simulations

Numerical simulations are now carried out considering different flow scenarios using a one-degree of freedom mechanical system. Spatial discretization is assumed to be associated with the fundamental vibration mode while the fourth order Runge–Kutta method is employed for time discretization. Therefore, the application of the Galerkin method reduces the system to a one-degree of freedom oscillator and the convergence analysis is restricted to time discretization, which points to time steps less than $\Delta_\tau = 7.3\times 10^{-5}$. All simulations consider the system parameters presented in Table 1, defined based

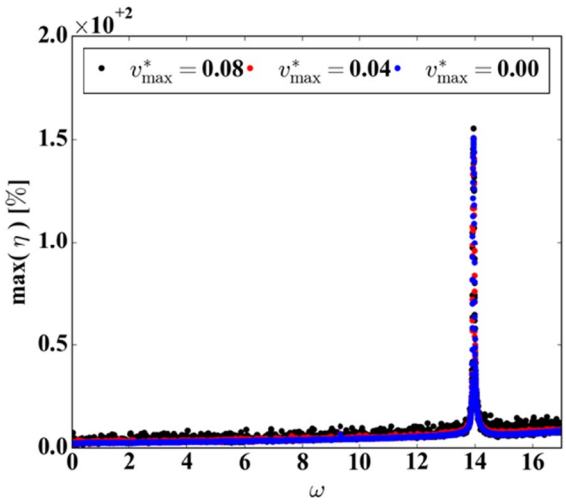

Fig. 7 Influence of the oscillation frequency considering a fluid described by a sinusoidal oscillation and stochastic fluctuation, relative maximum displacement. The amplitude displacement dispersion increases as the turbulence intensity rises

on typical geometrical dimensions for oil exploration together with information from Païdoussis [18].

Typical cases are of concern in order to verify the model ability to describe the Fluid-structure interaction. The constant flow speed is the standard case that usually appears in engineering applications involving pipe flows, being an important benchmark. A more realistic case considers a sinusoidal perturbed mean flow that can characterize the pumping of the fluid through different regions. Finally, a more sophisticated case represents the fluid flow from nonlinear oscillator that can capture more complex flows. It is noticeable that these cases present limit cycle behavior, being able to represent chaotic behaviors associated to situations related to instabilities and complex behaviors. In addition, each of these cases can incorporate velocity fluctuations, representing even more realistic flows where turbulence plays an important role. This is the case, for instance, in the gas and oil production stage where moderate to highly turbulent flows are found. Typically, a turbulent intensity of 8% of the mean flow velocity is considered high, whereas 4% is considered moderate.

On this basis, numerical simulations are split into three different cases discussed in the sequel: constant fluid flow speed; sinusoidal fluid flow; fluid flow represented by nonlinear oscillator. Each of these cases are treated considering two situations: with and without fluid velocity fluctuations.

3.1 Constant fluid flow velocity

Consider a pipe subjected to an internal flow with constant velocity. This is the case is usually associated with pipes without any obstacles, such as wall restrictions and valves, and no significant modification of flow trajectory. Under these conditions, it is not expected significant generation of different flow patterns rather than the formation of boundary layer. Typically, the increase of the flow velocity tends to induce vibrations with higher amplitudes. In this regard, a model verification is now of concern considering a constant flow $v = \overline{v}$ and assuming different levels between $\overline{v} = 1$ and $\overline{v} = 21$.

Figure 2 presents numerical simulations showed as time history of the structure displacement; the structure state space; and the maximum structure displacement as a function of the mean velocity. The increase of the mean flow velocity causes the increase of the structure oscillation amplitude, showing that at $\overline{v} = 21$, the maximum amplitude is 19.4% higher than the case where $\overline{v} = 1$, while for $\overline{v} = 9$ the maximum amplitude is 1.7% higher than in the case $\overline{v} = 1$. Besides, the increase of the mean flow velocity causes a reduction of structure frequency oscillation.

Turbulent flow is represented by incorporating a stochastic fluctuation on the fluid description by considering $v = \overline{v} + v^f$, assuming that v^* can vary from 0 to 8% of $\overline{v}$, which is varying from the deterministic case ($v^* = 0$) to high turbulent intensity. The inclusion of the velocity fluctuation brings new flow dynamics characterized by one of the most notorious turbulent patterns. Therefore, fluid flow in tubes and pipes subjected to different random oscillating frequencies is modeled to characterize the presence of any flow disturbance such as inner pipe obstacles, restrictions and expansions, and walls with high rugosity. Figure 3 presents numerical simulations for $\overline{v} = 21$ through the curve of maximum displacement amplitude as a function of turbulence intensity v^*. The idea is to show 10 simulations for each value of v^*, establishing a cloud of points that increases with the turbulent intensity. Each one of the simulations is different from each other due to random aspects. It should be noticeable that the case where $v^* = 0$ is the same result presented in Figure 2, without random aspects and $\overline{v} = 21$. When compared with the constant flow deterministic case, these results show that the

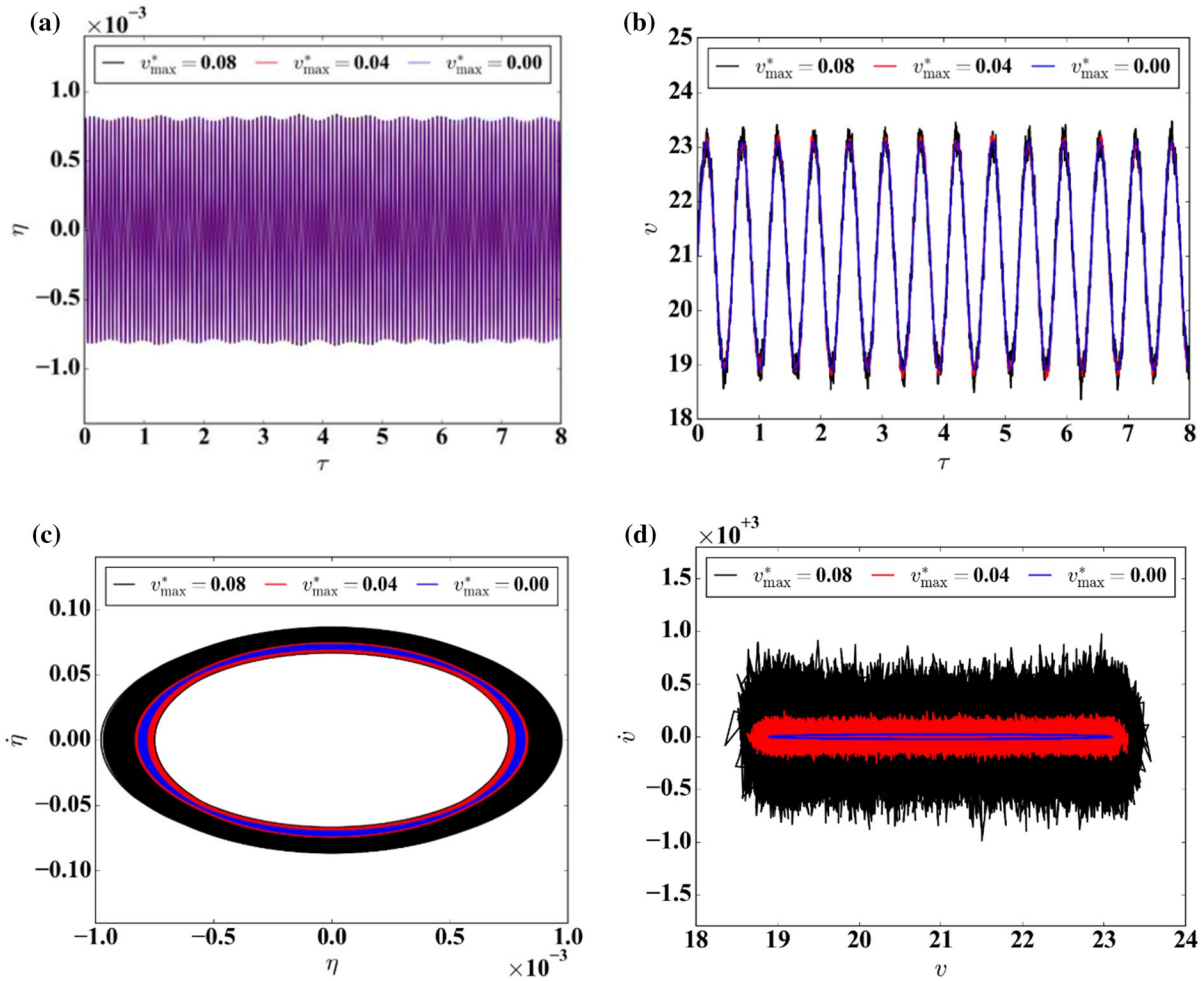

Fig. 8 Fluid-structure dynamical behavior considering a fluid described by a sinusoidal oscillation and stochastic fluctuation. **a** Time history of the structure displacement; **b** time history of the flow velocity; **c** structure state space; **d** flow velocity state space

stochastic fluctuation affects the displacement amplitude, which may vary between a decrease of 1% and an increase of 17.8%.

Figure 4 presents results for fluid flow mean velocity $\overline{v} = 21$ with stochastic fluctuation intensity of 0, 4 and 8% (without, moderate and high turbulent intensity), represented by the time history of structure displacement and the flow velocity, together with structure and fluid state spaces. By observing that $v^* = 0$ represents the deterministic case, it should be pointed out that the increase of the turbulent intensity significantly alters the fluid variables and the structure behavior, which means that turbulent flow has a great influence on the system response.

3.2 Sinusoidal fluid flow

Consider a pipe subjected to an internal flow with sinusoidal mean flow velocity, assuming that $v = \overline{v}(1 + a\sin(\omega\tau))$, which means that Fluid-structure analysis is decoupled. This test case introduces transient behavior of the fluid flow as a consequence of a fluid machinery such as pumps found in the gas and oil industry, being a more realistic model of the flow dynamics. Initially, a frequency curve is built considering maximum displacements evaluated with a slow quasi-static variation of frequency values. Figure 5 shows results of this case, establishing a comparison with the ones with the constant flow case ($a = 0$). It should be pointed out that sinusoidal

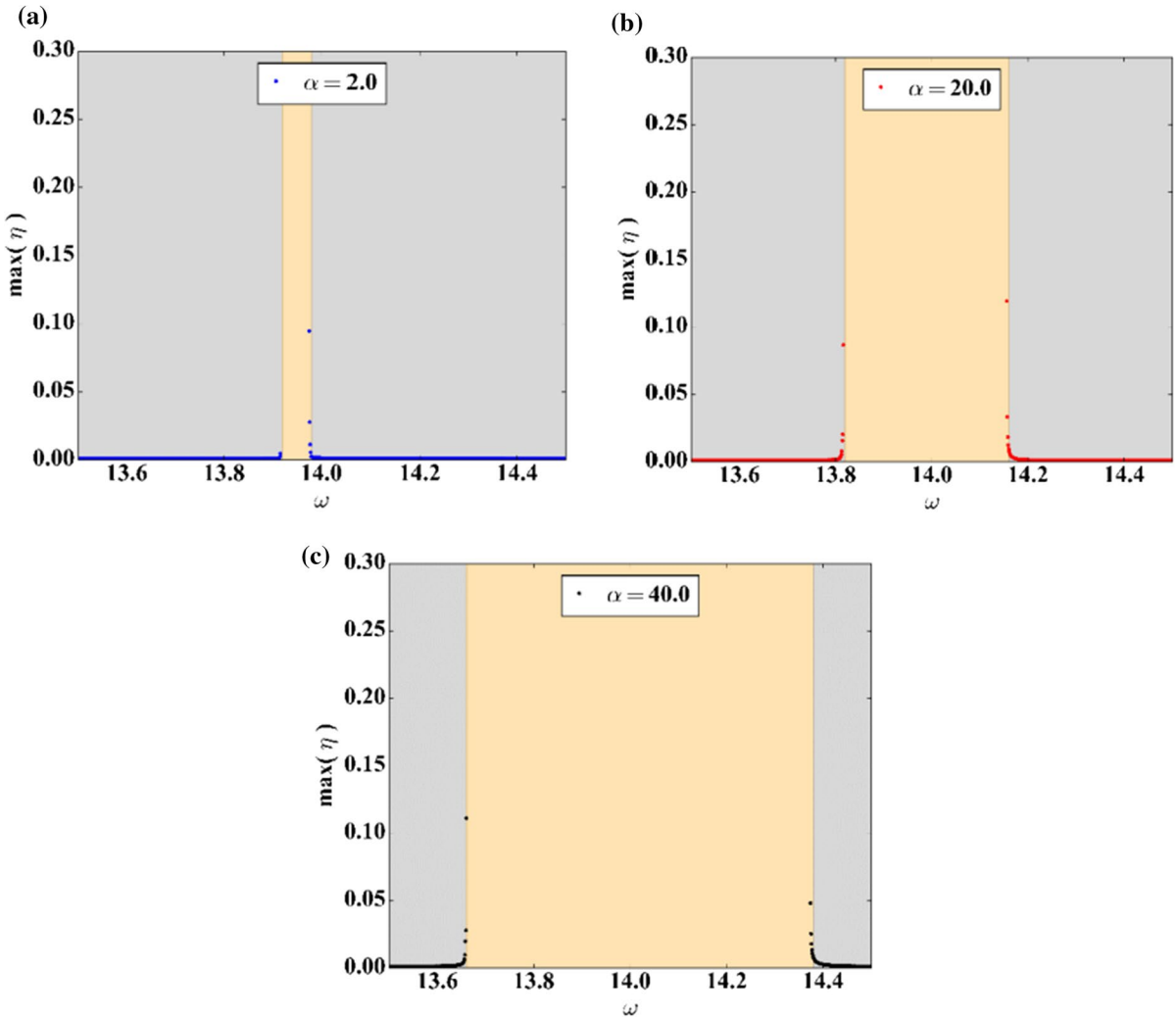

Fig. 9 Frequency analysis for different fluid characteristics and without nonlinear dissipation ($\chi = 0$), represented by maximum structure amplitude highlighting unstable (yellow) and stable (gray) regions. (**a**) $\alpha = 2.0$, (**b**) $\alpha = 20$ and (**c**) $\alpha = 40$

excitations promote a typical resonance phenomenon close to $\omega = 14$, which increases the maximum displacement of 80% in the case with $a = 0.08$ and of 20% in the case with $a = 0.04$.

Different situations are now treated considering $\overline{v} = 21$,$\omega = 10.75$ and distinct oscillation intensities,a: 0, 0.04 and 0.08. Figure 6 presents the time history of the structure displacement and flow velocity together with structure and fluid state spaces. The case with $a = 0$ does not have oscillation: $v = \overline{v}$. The increase of a causes the structure pulsation, which is represented by an oscillation that increases the amplitude together with the parameter value. Under these conditions, the structure amplitude is not altered in a significant way since it is far from the resonant condition.

The turbulent intensity is now of concern incorporating the stochastic fluctuation: $v = \overline{v}(1 + a\sin(\omega\tau)) + v^f$. Once again, this represent a turbulent pattern added to the main flow, providing a more accurate modeling of the profile generated by a fluid machinery such as a pump, which is likely to be turbulent due to strong fluid disturbance caused by flow trajectory modification and the presence of obstacles in the machinery. Frequency analysis is

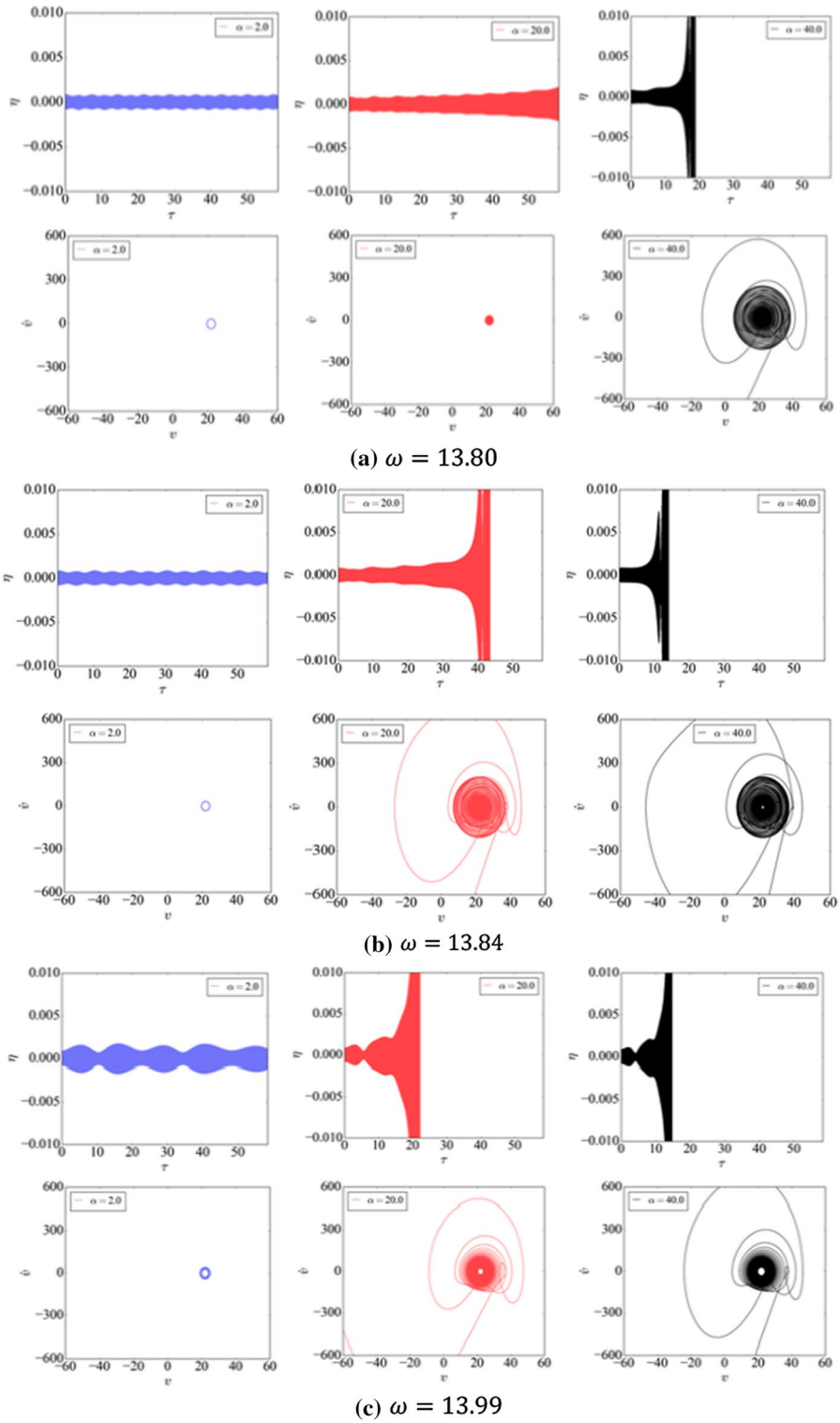

Fig. 10 Fluid-structure dynamical behavior with fluid described by a nonlinear oscillator without nonlinear dissipation ($\chi = 0$): left panel shows time history of the structure displacement while right panel shows the fluid state space. (**a**) ω = 13.80, (**b**) $\omega = 13.84$ and (**c**) $\omega = 13.99$

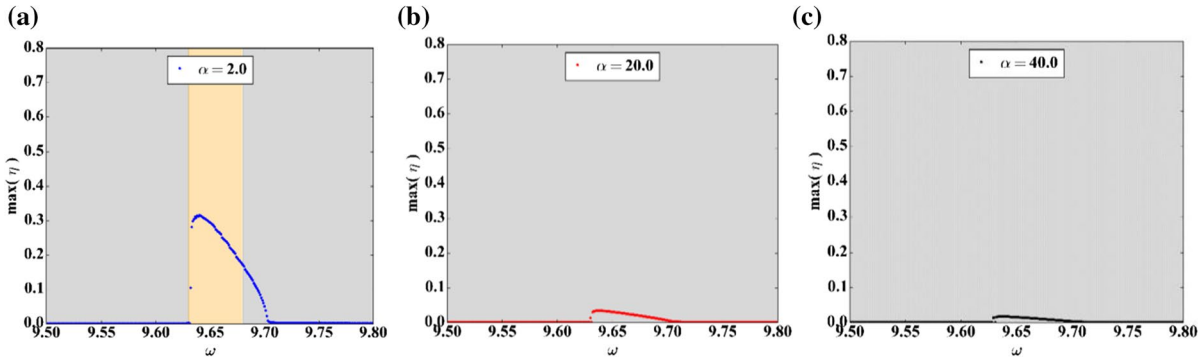

Fig. 11 Frequency analysis for different fluid characteristics and nonlinear dissipation of $\chi = 0.8$, represented by maximum structure amplitude highlighting unstable (yellow) and stable (gray) regions. (**a**) $\alpha = 2.0$, (**b**) $\alpha = 20$ and (**c**) $\alpha = 40$

presented in Fig. 7 by considering a turbulence intensity v^* that varies from 0 to 8% of the mean velocity $\overline{v} = 21$, representing the variation from deterministic to moderate and high turbulent intensity cases. Results show the same trend of the deterministic case, but with a displacement increase.

Figure 8 presents results for a specific case with $\omega = 10.75$ and $a = 0.1$, in the form of structure time history and flow velocity, and both the structure and fluid state spaces. Once again, results are characterized by random aspects, especially observed in the fluid variables, which changes the response compared with sinusoidal oscillation flow.

3.3 Fluid flow described by nonlinear oscillators

A more sophisticated fluid flow description is now of concern treating the case where the fluid flow is described by a nonlinear oscillator. This description is richer in a nonlinear dynamics perspective, being able to describe behaviors that are useful to represent some phenomena of the Fluid-structure interaction associated with instabilities and limit cycles.

In general, the route from laminar to turbulent flow passes to transition regions related to different patterns and three noticeable cases should be highlighted: wake transition; vortex breakdown; and the emergence of a thin viscous sublayer due to a no-slip boundary wall. Based on a nonlinear dynamics perspective, these transitions are associated with bifurcations that represents qualitative changes in the response structure. Nonlinear oscillators are able to capture such bifurcations, allowing a direct connection with expected fluid flow characteristics. Moreover, the continuous interaction between these patterns, from transitional to turbulent flow, may lead to the increasing of the structure fatigue, consequently, wall damage and failure of the fluid transport system, which makes this analysis an important issue.

Simulations related to the fluid flow governed by nonlinear oscillators are performed considering $\overline{v} = 21$; $a = 0.1$, and different levels of Fluid-structure coupling parameter, α: 2, 20, 40, representing the effects of the interaction between the flow patterns and the structure itself. Initially, it is considered a situation where fluid flow is represented by a linear oscillator, which means that nonlinear dissipation is neglected, $\chi = 0$. It is important to observe that Fluid-structure interaction is represented by an excitation provided by the structure response. Figure 9 presents frequency analysis for this case, identifying the region related to unstable responses (yellow region), evaluated by observing the general trend within the simulation period. Note that the increase of the parameter α that connects structure with fluid flow, increases the unstable region.

Details about the system response is presented in Fig. 10 in the form of time history of the structure displacement and the fluid state space. In this regard, structure behavior is represented by displacement while fluid behavior is represented by a state space composed by the fluid velocity and its time rate. Simulations are carried out in order to show different behaviors, including stable or unstable responses. Three test cases are treated for different frequency values, ω: 13.80; 13.84; 13.99. It is noticeable that the fluid flow described by nonlinear oscillators introduce different perspectives to the Fluid-structure

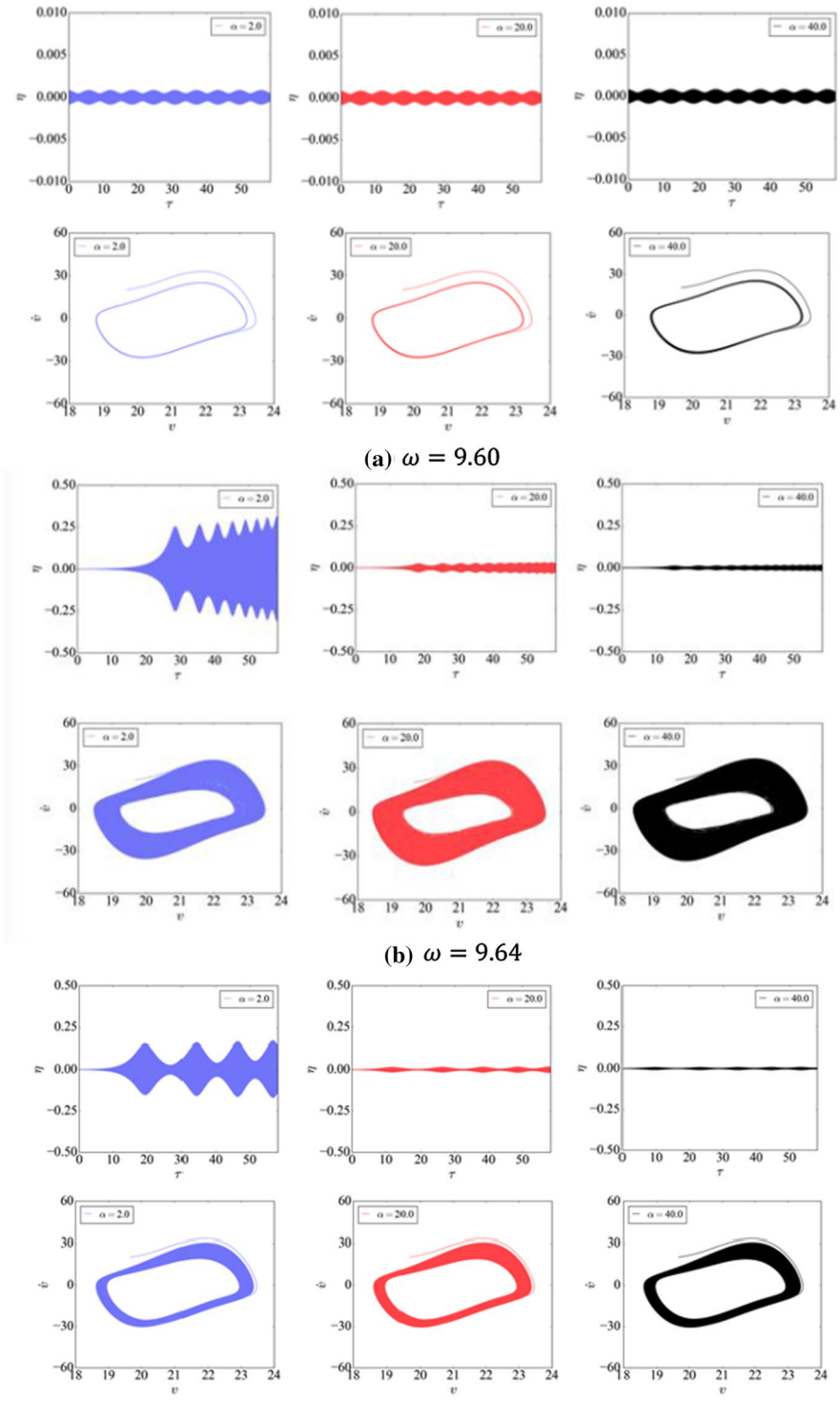

Fig. 12 Fluid-structure dynamical behavior with fluid described by a nonlinear oscillator with nonlinear dissipation $\chi = 0.8$: left panel shows time history of the structure displacement while right panel shows the fluid state space. (a)$\omega = 9.60$, (b) $\omega = 9.64$ and (c) $\omega = 9.68$

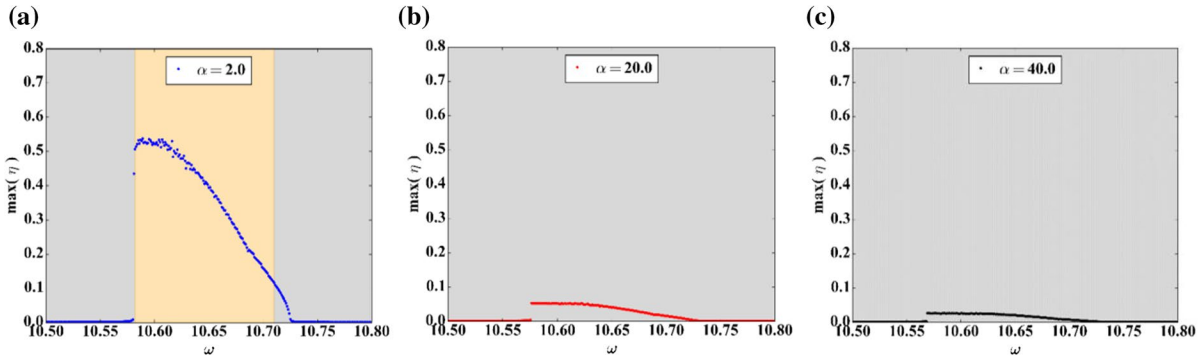

Fig. 13 Frequency analysis for different fluid characteristics and nonlinear dissipation of $\chi = 1.6$, represented by maximum structure amplitude highlighting unstable (yellow) and stable (gray) regions. (**a**) $\alpha = 2.0$, (**b**) $\alpha = 20$ and (**c**) $\alpha = 40$

interaction analysis. For all the three cases analyzed, there is a situation where unstable orbits promotes the system scape, causing an unstable structure behavior, which are essentially related to large structure amplitudes.

The effect of the nonlinear dissipation is now evaluated by considering the parameter $\chi = 0.8$, which means that fluid flow is represented by the oscillator nonlinear dynamics. Figure 11 presents the frequency analysis of this new situation for different values of the coupling parameter α, showing the nonlinear characteristic of the fluid description. Under these conditions, the increase of α reduces the unstable regions (yellow region in the figures) due to the nonlinear dissipation associated with the limit cycle characteristic of the nonlinear oscillator. Nevertheless, the frequency curve allows one to identify different branches that are essentially related to response patterns caused by the Fluid-structure interaction. Dynamical jumps should be pointed out as important aspect that characterizes the transition branches.

Figure 12 presents some results around the resonant peaks defined by three frequency values, ω: 9.60; 9.64; 9.68. When $\omega = 9.60$, the system presents a periodic response associated with a stable behavior for all treated values of α; when $\omega = 9.64$, results for $\alpha = 2$ has large oscillations associated with chaotic-like fluid behavior, presenting an unstable trend; by considering $\omega = 9.68$, structure oscillatory response is observed, and the unstable trend is not present anymore. Nevertheless, it is interesting to observe the different levels of amplitude responses for each one of the cases.

Fluid behavior is now altered by assuming an even higher nonlinear dissipation, $\chi = 1.6$. Figure 13 presents the frequency analysis showing that the unstable region is increased for low coupling parameters ($\alpha = 2$), but still similar for larger values of α. Note that this level of energy dissipation eliminates unstable regions for $\alpha = 20$ and $\alpha = 40$. Once again, dynamical jumps are defining different response branches that are ultimately related to fluid flow main aspects. Also interesting to note in Fig. 14a is the unstable region located at $\omega > 10.58$ and $\omega > 10.70$ that can potentially be related to fluid pattern transition when the onset of turbulence may occur, strongly affecting the structure response. On the other hand, the higher is the coupling parameter α the lower is the maximum the structure displacement η for the same frequency region.

Figure 14 highlights details of the system response observing three frequency values, ω: 10.55; 10.63; 10.73. For the case for $\omega = 10.55$, the system presents a periodic response associated with stable behavior for all treated values of the coupling parameters α; when $\omega = 10.63$ the system presents unstable behavior for $\alpha = 2$; when $\omega = 10.73$, the structure returns to the periodic stable response.

The turbulent effect is now of concern considering stochastic velocity fluctuations. Some of the previous cases are treated, which allows one to establish a comparison of its influence on the Fluid-structure interaction. The case considering the dissipation parameter $\chi = 0.8$ is treated as reference (previously discussed in Fig. 12). Under this assumption and incorporating stochastic fluctuations for v^* (varying

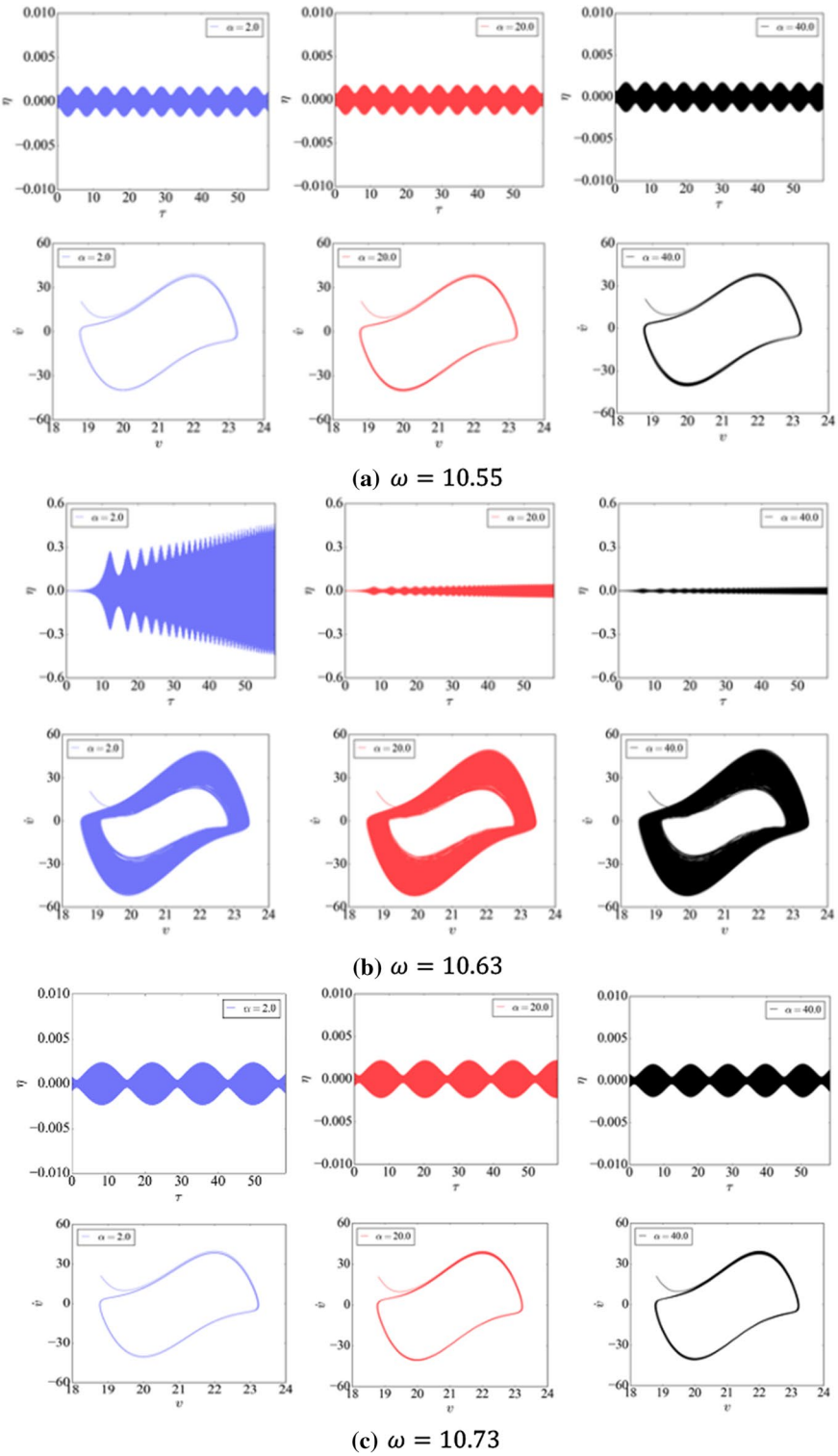

Fig. 14 Fluid-structure dynamical behavior with fluid described by a nonlinear oscillator with nonlinear dissipation $\chi = 1.6$: left panel shows time history of the structure displacement while right panel shows the fluid state space. (**a**) $\omega = 10.55$, (**b**) $\omega = 10.63$ and (**c**) $\omega = 10.73$

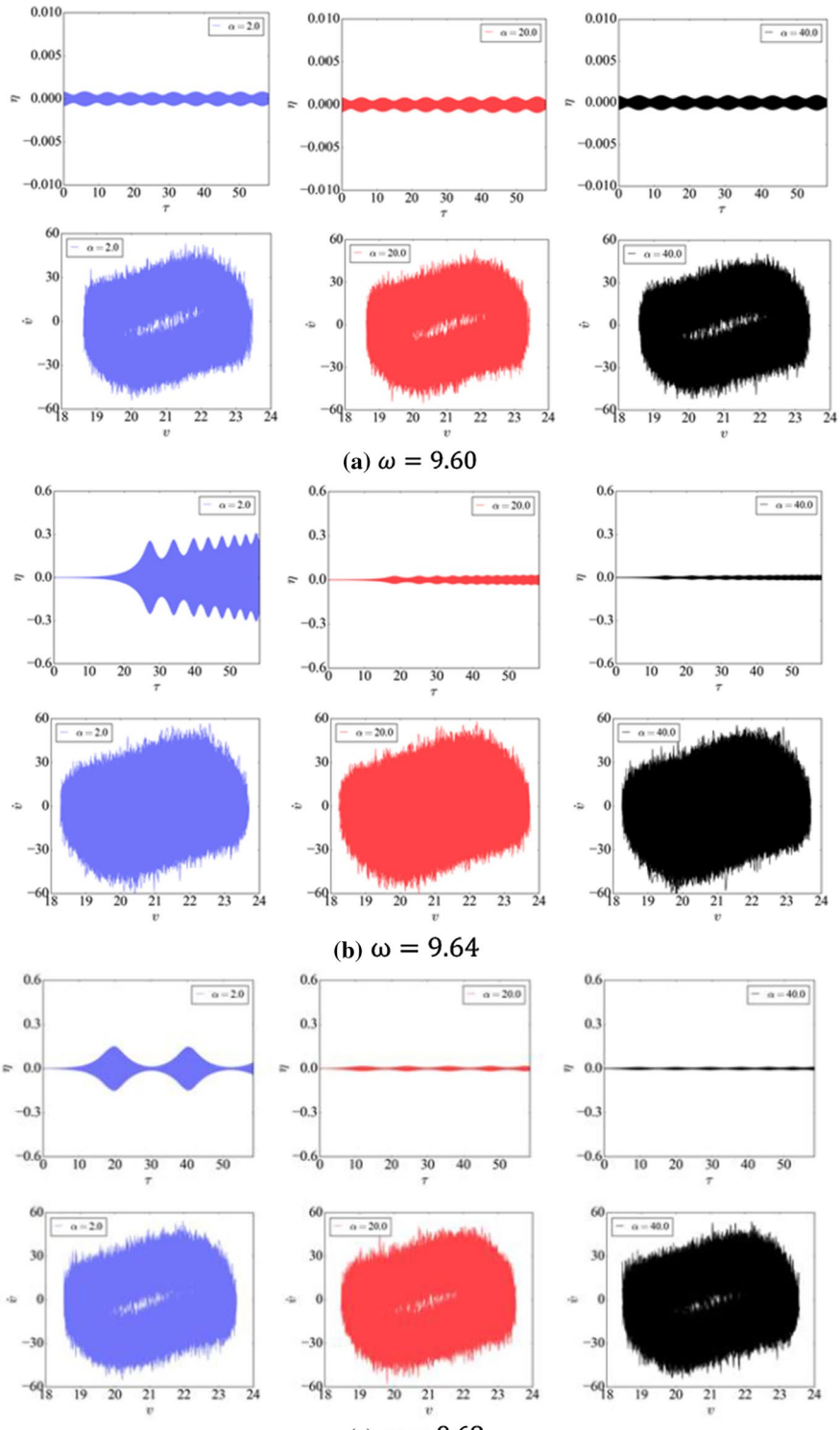

Fig. 15 Fluid-structure dynamical behavior with fluid described by a nonlinear oscillator with nonlinear dissipation $\chi = 0.8$ and stochastic fluctuations: left panel shows time history of the structure displacement while right panel shows the fluid state space. (**a**) $\omega = 9.60$, (**b**) $\omega = 9.64$ and (**c**) $\omega = 9.68$

from 0 to 8% of $\overline{v} = 21$: without, moderate and high turbulent intensity), Fig. 15 presents results related to these cases. It should be pointed out that the stochastic term does not alter the general stability trends but changes the system responses. Moreover, fluid flow dynamics is more irregular due to the presence of turbulent flow patterns, without a clear influence on the structure response. Therefore, it is possible to infer that the influence of turbulent flows in structure dynamics depends on important aspects such as the structure stiffness and Fluid-structure coupling.

4 Conclusions

This paper deals with the analysis of Fluid-structure interaction due to pipe internal flow using reduced-order models built by a combination of oscillators to describe either structure or fluid flow. Fluid flow is described by a combination of a nonlinear oscillator—a van der Pol oscillator with an excitation provided by the structure interaction, with stochastic turbulence model—the Langevin's equation. Initially, a model verification is performed considering simplified fluid flow characteristics represented by constant and sinusoidal fluid flow, with and without stochastic fluctuations. Afterward, fluid flow is governed by the nonlinear oscillator resulting in a rich Fluid-structure interaction dynamics represented by the limit cycle behavior. The use of nonlinear oscillator to model fluid flow brings new perspectives to the analysis of Fluid-structure interaction that can be interpreted by nonlinear dynamics perspective. Frequency response analysis allows the definition of stable and unstable responses, identified by branches associated with pattern transition regions. Dynamical jumps are other important transition characteristic that represent fluid flow behavior. The possibility of chaotic-like behaviors together with stochastic fluctuations furnishes richness to fluid representation, allowing a broader phenomenological description of Fluid-structure interactions. A comparison with experimental tests is necessary in order to define the range of applicability of the proposed model, but it shows an interesting potential.

Acknowledgements The authors would like to acknowledge the support of the Brazilian Research Agencies CNPq, CAPES and FAPERJ.

Declarations

Conflict of interest The authors declare that they have no conflict of interest.

References

1. Aranha JAP (2004) Weak three dimensionality of a flow around a slender cylinder: the ginzburg-landau equation. J Braz Soc Mech Sci Eng 26(4):355–367. https://doi.org/10.1590/S1678-58782004000400002
2. Bai Y, Xie W, Gao X, Xu W (2018) Dynamic analysis of a cantilevered pipe conveying fluid with density variation. J Fluids Struct 81:638–655. https://doi.org/10.1016/j.jfluidstructs.2018.06.005
3. Czerwi A (2018) Non-planar vibrations of slightly curved pipes conveying fluid in simple and combination parametric resonances. J Sound Vib 413:270–290. https://doi.org/10.1016/j.jsv.2017.10.026
4. El-Sayed TA, El-Mongy HH (2019) Free vibration and stability analysis of a multi-span pipe conveying fluid using exact and variational iteration methods combined with transfer matrix method. Appl Math Model 71:173–193. https://doi.org/10.1016/j.apm.2019.02.006
5. Franzini GR, Bunzel LO (2018) A numerical investigation on piezoelectric energy harvesting from vortex-induced vibrations with one and two degrees of freedom. J Fluids Struct 77:196–212. https://doi.org/10.1016/j.jfluidstructs.2017.12.007
6. Gonçalves RT, Franzini GR, Rosetti GF, Fujarra ALC, Nishimoto K (2012) Analysis methodology for vortex-induced motion (VIM) of a monocolumn platform applying the Hilbert-Huang transform. Offshore Mech Artic Eng. https://doi.org/10.1115/1.4003493
7. Gu J, Ma T, Duan M (2016) Effect of aspect ratio on the dynamic response of a fluid-conveying pipe using the Timoshenko beam model. Ocean Eng 114:185–191. https://doi.org/10.1016/j.oceaneng.2016.01.021
8. Korkischko IÃ, Meneghini JR (2010) Experimental investigation of flow-induced vibration on isolated and tandem circular cylinders fitted with strakes. J Fluids Struct 26(4):611–625. https://doi.org/10.1016/j.jfluidstructs.2010.03.001
9. Kurushina V, Pavlovskaia E, Postnikov A, Wiercigroch M (2018) Calibration and comparison of VIV wake oscillator models for low mass ratio structures. Int J Mech Sci 142–143:547–560. https://doi.org/10.1016/j.ijmecsci.2018.04.027
10. Loiseau J-C, Noack BR, Brunton SL (2018) Sparse reduced-order modelling: sensor-based dynamics to full-state estimation. J Fluid Mech 844:459–490
11. Lü L, Hu Y, Wang X, Ling L (2015) Dynamical bifurcation and synchronization of two nonlinearly coupled fluid-conveying pipes. Nonlinear Dyn 79:2715–2734. https://doi.org/10.1007/s11071-014-1842-y
12. Meng S, Kajiwara H, Zhang W (2017) Internal flow effect on the cross-flow vortex-induced vibration of a

cantilevered pipe discharging fluid. Ocean Eng 137:120–128. https://doi.org/10.1016/j.oceaneng.2017.03.055
13. Ni Q, Wang Y, Tang M, Luo Y, Yan H, Wang L (2015) Nonlinear impacting oscillations of a fluid-conveying pipe subjected to distributed motion constraints. Nonlinear Dyn 81:893–906. https://doi.org/10.1007/s11071-015-2038-9
14. Ni Q, Luo Y, Li M, Yan H (2017) Natural frequency and stability analysis of a pipe conveying fluid with axially moving supports immersed in fluid. J Sound Vib 403:173–189. https://doi.org/10.1016/j.jsv.2017.05.023
15. Ogink RHM, Metrikine A (2010) A wake oscillator with frequency dependent coupling for the modeling of vortex-induced vibration. J Sound Vib 329(26):5452–5473. https://doi.org/10.1016/j.jsv.2010.07.008
16. Orsino RMM, Pesce CP, Franzini GR (2018) Cantilevered pipe ejecting fluid under VIV : an investigation based on a planar nonlinear reduced-order model. J Braz Soc Mech Sci Eng. https://doi.org/10.1007/s40430-018-1467-z
17. Païdoussis MP, Luu TP, Prabhakar S (2008) Dynamics of a long tubular cantilever conveying fluid downwards, which then flows upwards around the cantilever as a confined annular flow. J Fluids Struct 24(1):111–128. https://doi.org/10.1016/j.jfluidstructs.2007.07.004
18. Païdoussis MP (2013) Fluid-structure interactions. Academic Press
19. Pavlovskaia E, Keber M, Postnikov A, Reddington K, Wiercigroch M (2016) Multi-modes approach to modelling of vortex-induced vibration. Int J Non-Linear Mech 80:40–51. https://doi.org/10.1016/j.ijnonlinmec.2015.11.008
20. Pope SB (1994) Lagrangian PDF methods for turbulent flows. Annu Rev Fluid Mech 26:23–63. https://doi.org/10.1146/annurev.fluid.26.1.23
21. Postnikov A, Pavlovskaia E, Wiercigroch M (2017) 2DOF CFD calibrated wake oscillator model to investigate vortex-induced vibrations. Int J Mech Sci 127:176–190. https://doi.org/10.1016/j.ijmecsci.2016.05.019
22. Ritto TG, Soize C, Rochinha FA, Sampaio R (2014) Dynamic stability of a pipe conveying fluid with an uncertain computational model. J Fluids Struct 49:412–426. https://doi.org/10.1016/j.jfluidstructs.2014.05.003
23. Sazesh S, Shams S (2019) Vibration analysis of cantilever pipe conveying fluid under distributed random excitation. J Fluids Struct 87:84–101. https://doi.org/10.1016/j.jfluidstructs.2019.03.018
24. Tang Y, Zhen Y, Fang B (2018) Nonlinear vibration analysis of a fractional dynamic model for the viscoelastic pipe conveying fluid. Appl Math Model 56:123–136. https://doi.org/10.1016/j.apm.2017.11.022
25. Ueno T (2019) Numerical investigations on passive supression of vortex-induced vibrations using non-linear vibration absorber: a wake-oscillator approach, MSc Dissertation, USP